



# Nanoparticle-mediated local delivery of methylprednisolone after spinal cord injury

Young-tae Kim<sup>1</sup>, Jon-Michael Caldwell, Ravi V. Bellamkonda\*

Neurological Biomaterials and Therapeutics, Laboratory for Neuroengineering, Wallace H. Coulter Department of Biomedical Engineering, Georgia Institute of Technology and Emory University, Atlanta, GA 30332, USA

## ARTICLE INFO

### Article history:

Received 22 September 2008

Accepted 30 December 2008

Available online 30 January 2009

### Keywords:

Nerve regeneration

Inflammation

Hydrogel

Drug delivery

## ABSTRACT

Systemic administration of a high-dose of Methylprednisolone (MP) can reduce neurological deficits after acute spinal cord injury (SCI). However, the use of high-dose MP in treating acute SCI is controversial due to significant dose related side effects and relatively modest improvements in neurological function. Here, using a rat model of SCI, we compare the efficacy of controlled, nanoparticle-enabled local delivery of MP to the injured spinal cord with systemic delivery of MP, and a single local injection of MP without nanoparticles. Based on histological and behavioral data, we report that local, sustained delivery of MP via nanoparticles is significantly more effective than systemic delivery. Relative to systemic delivery, MP-nanoparticle therapy significantly reduced lesion volume and improved behavioral outcomes. Nanoparticle-enabled delivery of MP presents an effective method for introducing MP locally after SCI and significantly enhances therapeutic effectiveness compared to bare MP administered either systemically or locally.

© 2009 Elsevier Ltd. All rights reserved.

## 1. Introduction

The loss of sensory, motor, and autonomic function after spinal cord injury (SCI) results from two major pathophysiological events: the initial injury and the subsequent secondary injury sequence triggered by the initial injury. The initial injury is acute and mainly caused by mechanical insult, such as forces of compression and displacement that rupture blood vessels and directly injure neurons and glia. The secondary injury is a subsequent degenerative response that includes edema, ischemia, inflammation, ionic imbalance (such as increased intracellular calcium), excitotoxicity, caspase and calpain activation, loss of energy metabolism, neurotransmitter accumulation, and apoptosis [1–3]. While the severity of the initial injury is dependent on the nature of trauma and cannot be controlled, the severity of the secondary injury may be modulated through the use of pharmacological agents such as Methylprednisolone (MP) or GM-1 [1]. The relatively slow progression of the secondary injury response (several hours to days after the initial injury) provides a therapeutic window and forms

the basis of the current clinical protocol for systemic administration of MP after SCI.

The synthetic glucocorticoid Methylprednisolone is the only FDA approved, clinically used agent for the treatment of acute SCI [4]. The Second National Acute Spinal Cord Injury Study demonstrated that the systemic administration of a high-dose (30 mg/kg bolus injection followed by a 5.4 mg/kg/h infusion over 23 h) regimen of MP during the first 8 h post-injury can reduce human neurological deficits after SCI [5]. Even though the underlying therapeutic mechanism is unclear, MP-mediated inhibition of lipid peroxidation and inflammatory response are thought to offer the main therapeutic benefits after SCI [6,7]. However, the use of systemic high-dose MP in acute SCI is controversial due to the risks of serious side effects, including gastric bleeding, sepsis, pneumonia, acute corticosteroid myopathy, and wound infection that accompany only modest improvements in neurological recovery [5,8–10]. We suggest that most of the side effects of MP therapy are related to the high systemic dosage and associated toxicity, and that the relatively modest neurological gains are a reflection of inefficient dosing to the injury site. Therefore, while MP has promise, its delivery to the injury site is likely the major impediment to its effective and widespread clinical use.

In this study, we investigate the use of nanoparticle-enabled sustained, site-specific MP delivery onto the injured spinal cord. This approach is designed to overcome the side effects of high-dose systemic dosage while significantly enhancing delivery efficiency.

\* Corresponding author. Wallace H. Coulter Department of Biomedical Engineering, Georgia Institute of Technology and Emory University, 313 Ferst Drive, Room 3108, Atlanta, GA 30332, USA. Tel.: +1 404 385 5038; fax: +1 404 385 5044.

E-mail address: [ravi@gatech.edu](mailto:ravi@gatech.edu) (R.V. Bellamkonda).

<sup>1</sup> Department of Bioengineering, University of Texas at Arlington, USA.

Biodegradable and injectable poly(lactic-co-glycolic acid) (PLGA)-based MP loaded nanoparticles (MP-NPs) carrying 1/20th (by weight) of the current clinical dose of MP were locally delivered at the site of injury in a dorsal over-hemisection model of SCI. While a contusion injured spinal cord model is more representative of SCI cases, the dorsal over-hemisection model was chosen in this study because it allows us to a) clearly distinguish the initial injury (caused by a direct incision) from subsequent secondary injury, and b) create a consistent and defined initial injury that minimizes variation from animal to animal.

The effect of MP-NP, systemic injection of MP (MP-sys), local injection of MP without nanoparticles – same dose as that encapsulated in NPs (MP-single injection), and nanoparticles with saline, but no MP (Saline-NP), on secondary injury was characterized both acutely and chronically. Acute analysis was performed 24 h after injury, and used to quantify the expression of proteins indicative of secondary injury: Calpain, iNOS, Bcl-2, and Bax. Chronic analysis was performed at 2 and 4 weeks after injury and used to quantify the severity of the wound-healing response, including lesion volume and injury-related cellular reactivity. In addition, the functional recovery of the animals was assessed by behavioral examination. These results were quantified and compared to both Saline-NP-treated control animals (Saline-NP) and systemically administrated MP (30 mg/kg, single dose) animals (MP-sys).

## 2. Materials and methods

### 2.1. Fabrication of MP nanoparticles

The Methylprednisolone (MP)-encapsulating poly(lactic-co-glycolic acid) (PLGA)-based nanoparticles (MP-NPs) were fabricated by modification of the double emulsion (water/oil/water phase) method as described in Li et al. [11]. To allow for sustained MP delivery (3–4 days) onto the injured spinal cord, such that it overlaps with the critical period for secondary injury treatment (the first 3–4 days), relatively fast degrading PLGA (50:50) NPs were used. Briefly, 2% (w/v) PLGA copolymer (50:50, Polysciences) was dissolved in methylene chloride (Fisher Scientific), and MP sodium succinate (15 mg, Pharmacia) was dissolved in sterilized, deionized water (250 µl). The MP solution was then added into 5 ml of ice-cooled PLGA solution. The MP solution was emulsified three times in PLGA copolymer solution by homogenization at 4000 rpm (13 s/run). This emulsion was then added into poly(vinyl alcohol) (PVA, 87–89% hydrolyzed, Aldrich) solution (0.4% (w/v)) in sterilized deionized water and homogenized three times at 7000 rpm (18 s/run). This double emulsion was diluted in 0.1% PVA solution, and methylene chloride was removed by evaporation in a vacuum chamber for 3 h with moderate stirring. The MP-NPs in 0.1% PVA solution were collected by centrifugation at 8500g for 15 min and washed twice with sterilized deionized water before lyophilization. The lyophilized MP-NPs were stored at –20 °C. All described procedures were performed under sterile conditions. The size of the NPs was measured by scanning electron microscopy (S-800 SEM, Hitachi). The MP encapsulation efficiency was determined through the quantitative comparison of the amount of MP between initial loading and the MP remaining in the 0.1% PVA solution after centrifugation of the MP-NPs. The amount of MP was determined through UV spectroscopy (at 247 nm, BIO-TEK). The saline-encapsulating NPs (Saline-NPs) were fabricated as an experimental control. The fabrication procedure for these control nanoparticles was exactly the same as that for the MP-NPs, except that sterilized saline was encapsulated instead of MP.

### 2.2. *In vitro* MP release profile and bioactivity

The *in vitro* release profile was examined to characterize MP released from the NPs as a function of time. To replicate the MP release inside spinal cord tissue, the MP-NPs (2 mg, lyophilized powder) were embedded into a 0.6% agarose gel (Cambrex) [12] and were incubated with phosphate buffered saline (PBS, pH = 7.4) at 37 °C. The Saline-NPs were also embedded into identical gels as a control. The supernatant was collected at 24, 48, 72, and 96 h after incubation, and the amount of MP released from the NPs at different incubation times was determined through UV spectroscopy (at 247 nm, BIO-TEK).

The bioactivity of the released MP was examined by co-incubation with lipopolysaccharide (LPS, Sigma)-stimulated primary rat microglia and quantifying their nitric oxide (pro-inflammatory factor [13]) release. The primary microglia were harvested from postnatal day 3 rat pups as described in Giulian et al. [14]. Two weeks after initial mixed seeding, the microglia were mechanically harvested (through vigorous agitation overnight on an orbital shaker) and seeded on poly-L-lysine (0.1 mg/ml, Sigma) pre-coated tissue culture plates. Two days after seeding the microglia, they were separated into two different groups: one group was co-

cultured with the MP-NPs (2 mg of NPs – the same amount of *in vivo* delivered MP-NPs) embedded 0.6% agarose gel, and the other group was co-cultured with Saline-NP embedded 0.6% agarose gel. The microglia were then stimulated by LPS (5 ng/ml) to release nitric oxide, and the amount of nitric oxide was measured at 24, 48, and 72 h by Griess Reagent System (Promega).

### 2.3. Preparation of MP-NP and Saline-NP solutions for local delivery

The sterilized and lyophilized MP-NPs and Saline-NP were prepared by suspending them in sterilized PBS just before use. MP-NP and Saline-NP solutions (each with 1 mg of NPs suspended in 5 µl PBS) were stored at 4 °C until use. The 1 mg of MP-NPs' lyophilized powder contained approximately 200 µg of MP (based on an estimated 65% encapsulation efficiency of the nanoparticles).

### 2.4. Preparation of MP-NP and Saline-NP embedded agarose gels

The agarose gels that embed the NPs were made of 0.6% (w/v) agarose gel (Cambrex) in 1 × PBS. This solution was mixed well with 1 mg of NPs and allowed to cool at 4 °C for 30 min. The denser upper layer of gel that was used to hold the NP embedded gel *in vivo* was a solution of 0.7% (w/v) agarose gel (Cambrex) in 1 × PBS. Total amount of delivered MP was approximately 400 µg (i.e., 200 µg as a solution and 200 µg as an embedded gel).

### 2.5. Local delivery of MP-NPs onto the dorsal over-hemisection spinal cord injury

All procedures were conducted according to Institutional Animal Care and Use Committee (IACUC) approved protocols. Adult male rats ( $n = 36$ , 230–260 g, Sprague-Dawley, Harlan) were induced to anesthetic depth with inhaled isoflurane at 3–4%. Throughout the surgery, the animal was maintained at 1.5–2% isoflurane. Before surgery, the surgical area was shaved and the incision site cleansed with a chlorohexiderm scrub. The ninth or tenth thoracic spinal cord segments (T9–10) were exposed by laminectomy. The dorsal over-hemisection was performed by coronally severing at 1.5 mm depth and 2 mm width, using fine microscissors previously marked at a depth of 1.5 mm. The MP-NP solution (5 µl, 200 µg MP/animal,  $n = 17$ ) was then loaded into a sterilized 26G Hamilton syringe and topically delivered onto the lesion site. After delivering the MP-NP solution, the MP-NP embedded agarose gel (containing approximately 200 µg MP/animal) was placed directly onto the injury site. The MP-NP embedded gel was secured by applying a liquid state of the denser agarose gel, which was quickly solidified by local cooling as described in Jain et al. [15] (Fig. 1B). Both a solution of Saline-NP and an agarose gel with embedded Saline-NPs were topically delivered onto the exposed lesion site ( $n = 19$ ). After delivering the MP-NPs or Saline-NPs, the muscle and skin were closed in layers. The animals recovered on a heating pad. Animals were monitored regularly and their bladders were manually expressed throughout the survival period until reflex voiding was established.

### 2.6. Systemic delivery of MP (MP-sys) into dorsal over-hemisection spinal cord injury

All surgical procedures were the same as for the local delivery of MP-NPs except that the MP was not encapsulated by NPs but was instead delivered systemically through intravenous administration. The MP was dissolved in sterilized saline (30 mg/kg body weight, 7–8 mg MP/animal) and was administered 5 min after surgery through a tail vein. The animals ( $n = 15$ ) were monitored as described above.

### 2.7. Local delivery of single dose MP (Single-MP) onto dorsal over-hemisection spinal cord injury

To distinguish between the benefits of one-time local delivery versus sustained local delivery enabled by NPs, unencapsulated, free MP (400 µg MP in 10 µl saline/animal,  $n = 4$ ) was directly delivered onto the lesion site. Care was taken to ensure that all surgical procedures were the same as those used for local delivery of MP-NPs.

### 2.8. Behavioral assessment

Prior to surgery, animals were evaluated to establish baseline behavior. The behavior of the MP-NP, Saline-NP, and MP-sys-treated animals was measured at 1, 2, and 4 weeks after surgery. Grid walking and beam walking tests were used to evaluate sensory-motor functional recovery after spinal cord injury. In both walking tests, the number of tested animals was as follows: MP-NP ( $n = 8$  for 1 week,  $n = 17$  for 2 weeks, and  $n = 7$  for 4 weeks); MP-sys ( $n = 5$  for 1 week,  $n = 10$  for 2 weeks, and  $n = 7$  for 4 weeks); and Saline-NP ( $n = 5$  for 1 week,  $n = 10$  for 2 weeks, and  $n = 10$  for 4 weeks). We slightly modified the protocol described in Kunkel-Bagden et al. [16]. Briefly, the animals were trained to walk on a metal wire grid (50 cm × 30 cm, 2 cm = distance between wires in the grid) and across a narrow metal beam (1 m long and 3 cm wide). In the wire grid tests, the number of hindlimb slips below the plane of the wire grid over a span 2 min was counted. In the beam walking tests, the number of hindlimb slips off the beam while animals traversed the beam was counted.

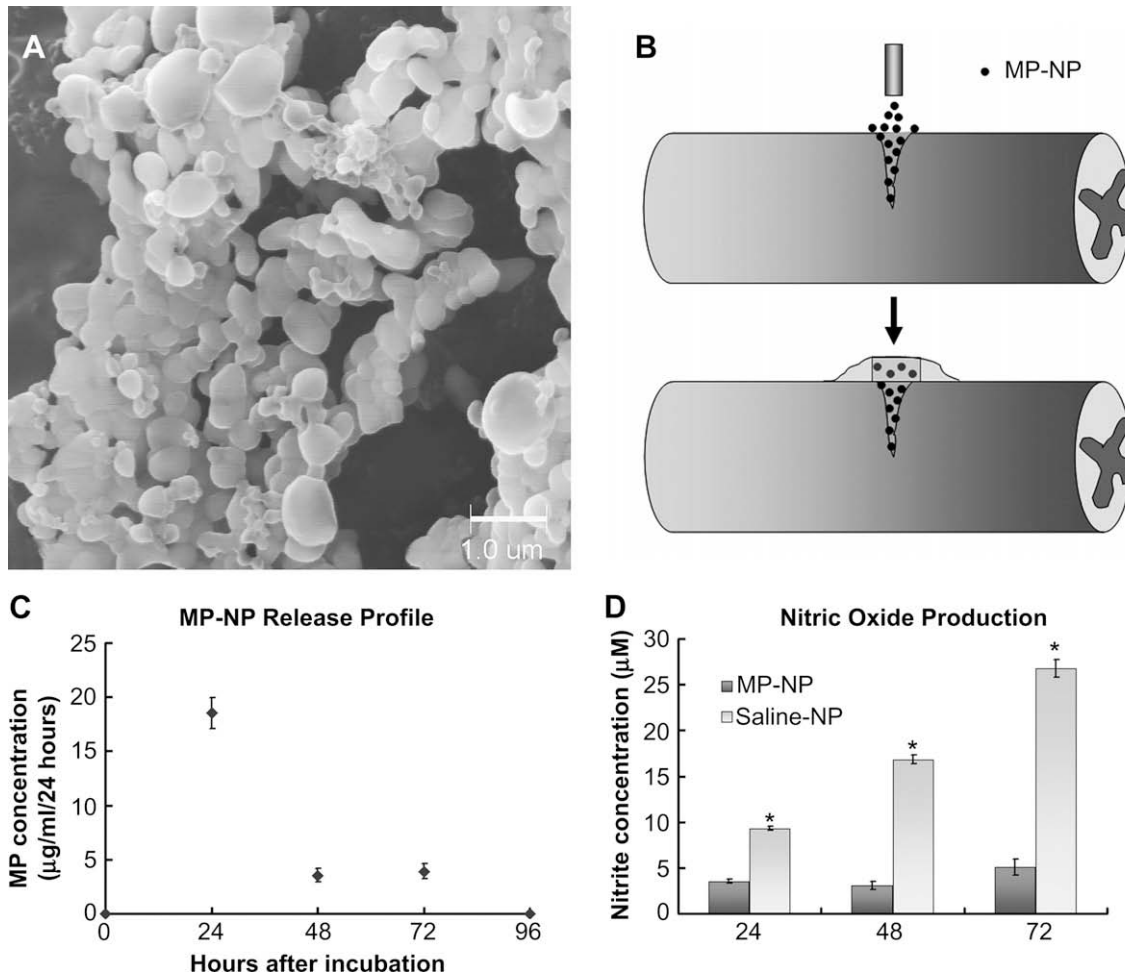


**Fig. 1.** Methylprednisolone-encapsulating PLGA nanoparticles (MP-NP). A) An SEM image of the lyophilized MP-NPs. Scale bar = 1 μm. B) Schematic of topical and local delivery of the MP-NPs onto dorsal over-hemisection lesioned spinal cord (see Section 2). C) MP-NP release profile over 4 days at 37 °C in saline. D) Quantitative comparison of amount of released nitrite from reactive microglia when exposed to MP-NPs and Saline-NPs. The co-incubation of MP-NPs with reactive microglia significantly suppresses nitric oxide production by reactive microglia. Error bars represent s.e.m. \* $P < 0.05$ .

### 2.9. Acute spinal cord reactivity after 24 h injury

To examine the therapeutic effects of delivered MP (by local or systemic delivery) on markers of secondary injury, the animals ( $n = 4$  for each condition: MP-NP, Saline-NP, Single-MP, and MP-sys) were perfused at 24 h after hemisection injury. Intact (i.e., normal) animals served as a positive control. Serial sections (longitudinally cryosectioned, 16 μm thick) were incubated overnight at 4 °C with the following primary antibody solutions: Calpain (1:500, mouse IgG1, Sigma), inducible nitric oxide synthase (iNOS, 1:500, rabbit IgG, Sigma), Bcl-2 (1:100, rabbit IgG, Santa Cruz), Bax (1:100, rabbit IgG, Santa Cruz), NeuN (1:200, mouse IgG1, Chemicon), NF160, and GFAP. In addition, injured spinal cords from different animals for each experimental condition (at 24 h after injury) were dissected and prepared for Western blot analysis.

### 2.10. Tissue preparation and histological analysis of spinal cord tissue reactivity

At 2 and 4 weeks after injury, the animals (MP-NP, Saline-NP, and MP-sys-treated,  $n = 5$  animals for each condition and time point) were perfused transcardially with PBS followed by 4% paraformaldehyde in PBS. The animals treated with Single-MP were perfused only at two weeks after injury. The spinal cords were removed and post-fixed overnight in the same fixative. Longitudinal 16 μm thick tissue sections were cryosectioned. Serial longitudinal sections were collected from each specimen and processed for a particular antigen or antigen pair using immunohistochemical methods. Serial sections were incubated with the following primary antibody solutions overnight at 4 °C: glial fibrillary acidic protein (GFAP, 1:1000, rabbit IgG, DakoCytomation) to identify astrocytes, ED-1 (1:1000, mouse IgG1, Serotec) to identify macrophage/reactive microglia, neurofilament 160 kDa (NF160, 1:500, mouse IgG1, Sigma) to identify the axons, and CS-56 (1:250, mouse IgM, Sigma) to identify the chondroitin sulfate proteoglycan (CSPG) molecules.

Secondary antibodies diluted 1:220 in 0.5% Triton in PBS included goat anti-rabbit IgG (H + L) Alexa 594 (Invitrogen) for GFAP, goat anti-mouse IgG1 Alexa 488 for NF160 and ED-1, and goat anti-mouse IgM Alexa 488 for CS-56. Sections treated only with secondary antibody but with no primary antibody were used to determine non-specific binding.

### 2.11. Semi-quantitative immunofluorescence analysis for assessing spinal cord tissue reactivity

For a semi-quantitative comparison of the tissue reactivity at the injured spinal cord between experimental groups at different time points (i.e., 24 h, 2 weeks, and 4 weeks), the immunostained images were captured with an Olympus digital camera and their immunostaining intensity was quantified, averaged, and compared using a custom MatLab (Mathwork)-based image analysis program created in our laboratory as described in Jain et al. [15]. While several other methods, including Western blot or Chemiluminescent quantification [17], are currently available to quantify/semi-quantify a protein expression, the semi-quantitative immunofluorescence analysis was chosen in this study because it allows us not only to semi-quantify the expression level of each protein, but also to determine the spatial distribution, specially at lesion site, of each protein.

For GFAP and CS-56 quantification, this program generated line profiles (40 line profiles/image) and extracted relative fluorescent intensity as a function of distance from the lesion interface (delineated by GFAP<sup>+</sup> glial scar). All images were taken at the same exposure time and conditions. For each stained image, a reference line (i.e., 0 μm distance) was generated at the lesion interface and then 40 line profiles were generated. An average intensity profile for each staining was calculated by averaging the coinciding increments of the 40 line profiles and displayed by an average intensity profile versus distance from the lesion interface. A minimum of 60 images (GFAP) and 36 images (CSPG) for each experimental group and time point ( $n = 5$

animals) were used to obtain the overall average intensity profiles of each staining. The overall average intensity profiles for both GFAP and CS-56 as a function of distance from the lesion interface were compared between experimental groups. For statistical analysis, the area under the curve of the overall average intensity profiles was determined for three different distances: 0–100  $\mu\text{m}$ , 100–300  $\mu\text{m}$ , and 300–500  $\mu\text{m}$  from the interface.

For Calpain, iNOS, Bcl-2, and Bax quantification, the image analysis program generated line profiles (40 line profiles/image, Fig. 2A and B), extracted relative fluorescent intensity, and averaged each one to create an average intensity profile (Fig. 2B inset). The average intensity profile was then averaged again to generate a representative quantitative intensity per image. A minimum of 44 images (i.e., 44 representative quantitative intensities) for each experimental group ( $n = 4$  animals) were used to obtain the overall average intensity for each staining, and this overall average intensity was compared between experimental groups.

For ED-1<sup>+</sup> cell counting, the ED-1<sup>+</sup> immunostained images were captured at the lesion site and the number of ED-1<sup>+</sup> cells/mm<sup>2</sup> was determined using Image-pro plus software and compared between experimental groups.

For lesion volume quantification, the GFAP immunostained images were captured (a minimum of 24 images per each animal,  $n = 5$  animals for each experimental group and time point). The lesion area (i.e., lesion core) was delineated by GFAP<sup>+</sup> glial scar (Fig. 3B). The lesion area/image was quantified by Image-pro plus software, multiplied by tissue thickness, and then added to generate the lesion volume. The measured lesion volume was averaged and compared between experimental groups at two different time points: 2 and 4 weeks after injury.

2.12. Statistical analysis

An ANOVA, Tukey post hoc test was used to calculate the significance of differences between mean values. A  $p$  value less than 0.05 was considered statistically significant.

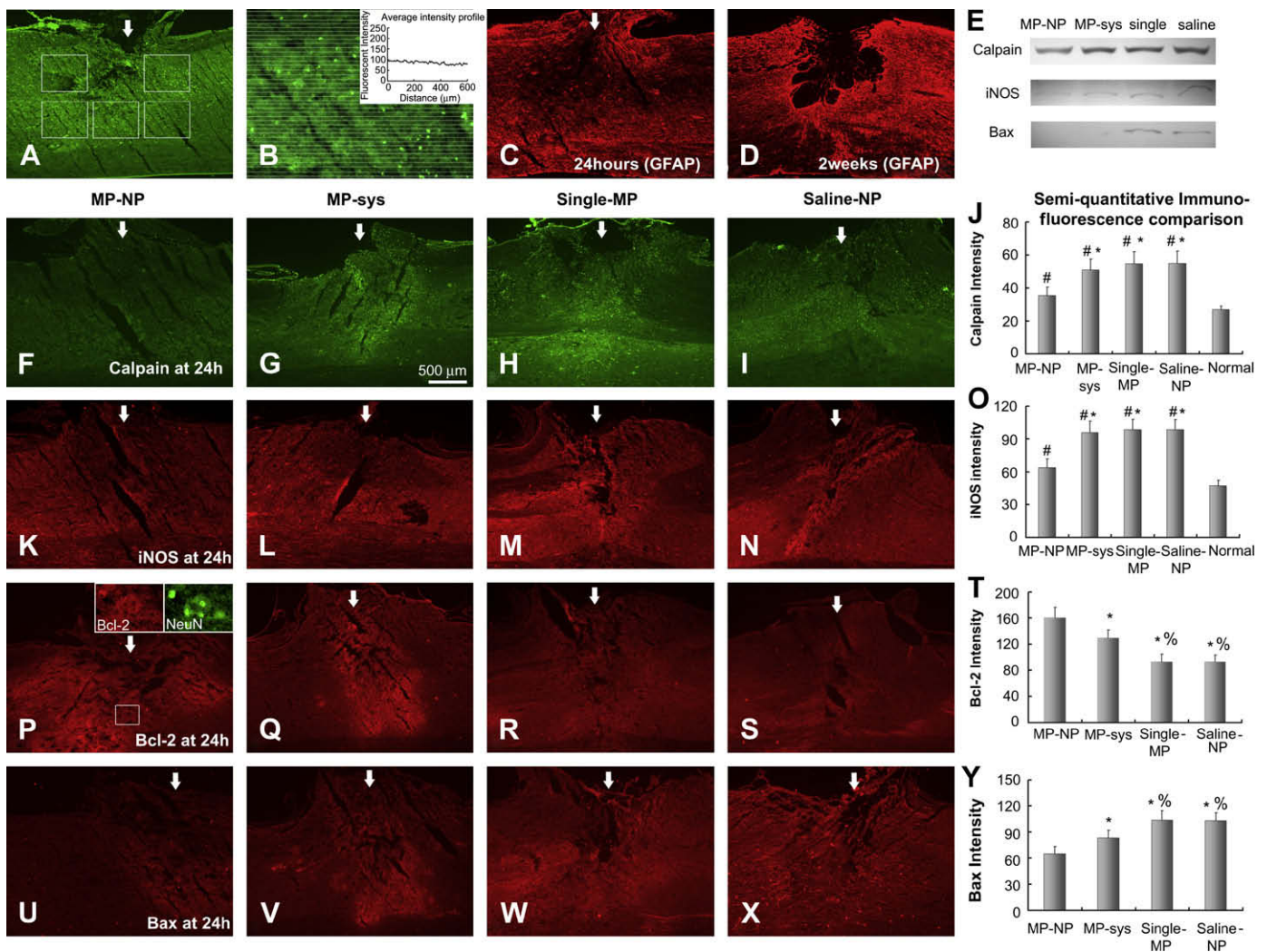


**Fig. 2.** Acute therapeutic effects of MP-NPs on hemisectioned spinal cord, 24 h after treatment. A, B) Semi-quantitative immunofluorescence analysis used for the semi-quantitative analysis of the lesioned spinal cord reaction (see Section 2). (A) Representative longitudinally sectioned and Calpain-immunostained spinal cord tissue. The immunofluorescence images (i.e., white boxes) were taken from around the incision site, indicated by a white arrow. (B) One of the images from (A). For each image, forty intensity line profiles were generated and averaged to create an average intensity profile (inset). The average intensity profile was then averaged again to generate a representative quantitative intensity per image. C, D) Comparison of GFAP, a marker for astrocytes, within an immunostained spinal cord tissue between 24 h (C) and 2 weeks (D) after injury. These two representative figures were from the Saline-NP-treated animals. The arrow indicates the incision site. E) The results of Western blot analysis for Calpain, iNOS, and Bax between experimental groups. Abbreviation: Single = Single-MP and Saline = Saline-NP. F–I) Representative (longitudinally sectioned) Calpain-immunostained spinal cord tissue at 24 h after injury: (F) MP-NP, (G) MP-sys, (H) Single-MP, and (I) Saline-NP-treated animal. White arrows indicate incision sites. (J) A quantitative comparison of the intensity of Calpain at 24 h after injury. K–N) Representative iNOS immunostained spinal cord tissue at 24 h after injury: (K) MP-NP, (L) MP-sys, (M) Single-MP, and (N) Saline-NP. (O) A quantitative comparison of the intensity of iNOS at 24 h after injury. P–S) Representative Bcl-2 immunostained spinal cord tissue at 24 h after injury: (P) MP-NP, (Q) MP-sys, (R) Single-MP, and (S) Saline-NP. (T) A quantitative comparison of the intensity of Bcl-2 at 24 h after injury. Inset figures in (P) are double immunostained for Bcl-2 (red) and NeuN (green), showing the highly increased expression of the Bcl-2 around Neurons. U–X) Representative Bax immunostained spinal cord tissue at 24 h after injury: (U) MP-NP, (V) MP-sys, (W) Single-MP, and (X) Saline-NP. (Y) A quantitative comparison of the intensity of Bax at 24 h after injury. Error bars represent s.e.m. # $P < 0.05$  between normal and others. \* $P < 0.05$  between MP-NP and others. % $P < 0.05$  between MP-sys and others (i.e., Single-MP and Saline-NP).

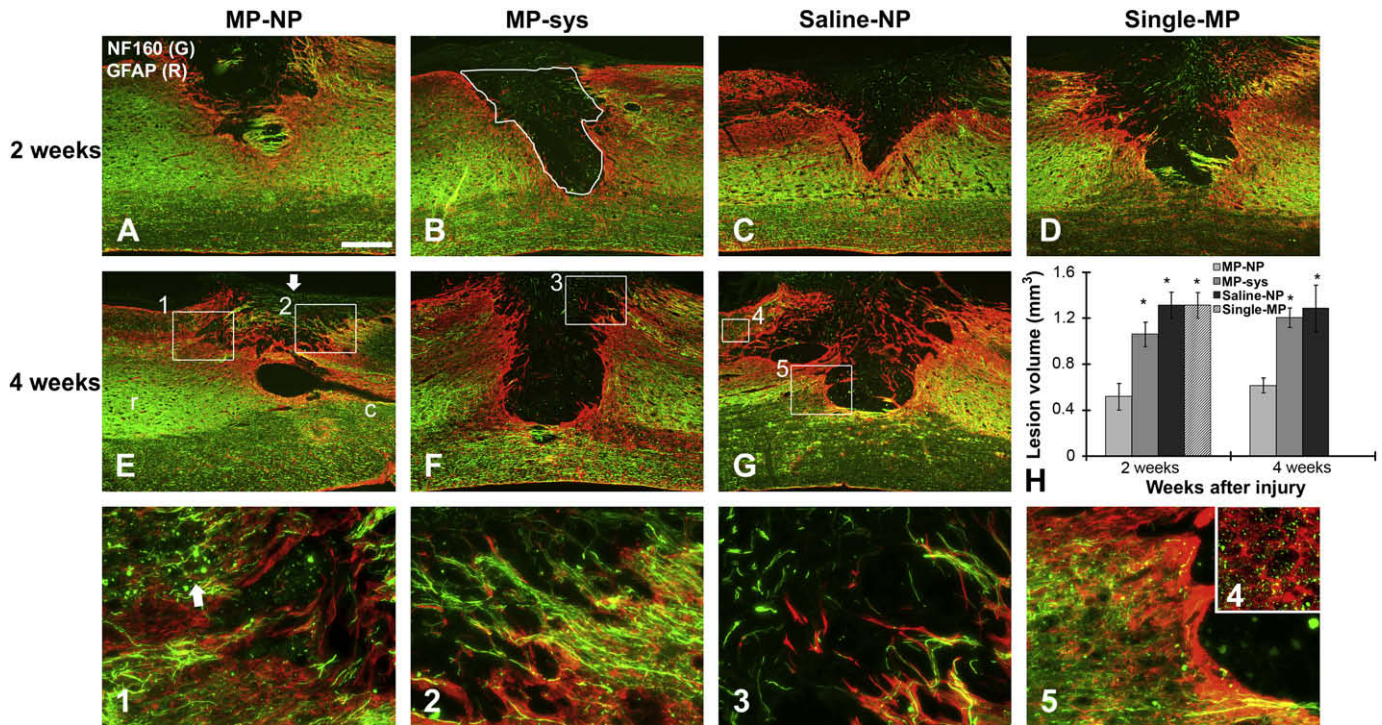


**Fig. 3.** Significantly reduced lesion volume from MP-NP local treatment. A–D) GFAP (a marker for astrocytes, red) and NF160 (a marker for axons, green) double immunostained (longitudinally sectioned) spinal cord tissue at the lesion site 2 weeks after injury: (A) MP-NP, (B) MP-sys, (C) Saline-NP, and (D) Single-NP-treated animals. Scale bar = 500  $\mu$ m. White line in (B) shows the lesion area. E–G) GFAP and NF160 double immunostained spinal cord tissue at the lesion site 4 weeks after injury: (E) MP-NP, (F) MP-sys, and (G) Saline-NP-treated animals. Numbered images (1–5) are magnified and from (E–G). The arrow in (E) indicates NF160<sup>+</sup> axons observed at the dorsal surface of the lesion site in MP-NP-treated animals. The arrow in (1) indicates the NF160<sup>+</sup> axons observed at the dorsal rostral to the lesion site. Image (4) shows the fragmented NF160<sup>+</sup> axons in the dorsal rostral to the lesion site (Saline-NP-treated animal, G). The arrow in (E) indicates NF160<sup>+</sup> axons observed at the dorsal surface of the lesion site in MP-NP-treated animals. H) A quantitative comparison of the lesion volume (delineated by GFAP<sup>+</sup> astroglial scar, see Section 2) at two different time points: 2 weeks and 4 weeks after injury. Compared to Saline-NP-treated animals, the lesion volume is significantly reduced at both 2 weeks and 4 weeks after injury by MP-NP local treatment, but not by either a systemically delivered high-dose of MP (MP-sys) or a single local injection of unencapsulated MP (Single-MP). Error bars represent s.e.m. \* $P < 0.05$  between MP-NP and others. Abbreviation: r = rostral and c = caudal stump.

### 3. Results

#### 3.1. Fabrication and *in vitro* characterization of MP-NPs

Biodegradable PLGA-based nanoparticles were used to encapsulate and slowly release MP. The fabricated MP-NPs (submicron scale: 200–700 nm in diameter) were sterilized and stored as a lyophilized powder (Fig. 1A). The MP encapsulation efficiency was determined to be 65% (see Section 2). The MP-NPs were later mixed in saline solution where they formed spheres (as opposed to large aggregates in a lyophilized powder), enabling localized and topical delivery onto the lesion site via a Hamilton syringe needle (Fig. 1B). Following an initial burst at 24 h after incubation, the MP was slowly released from the NPs over 4 days at 37 °C *in vitro* (Fig. 1C). The released MP was bioactive and significantly suppressed nitric oxide (pro-inflammatory factor) production from LPS-stimulated reactive primary rat pup-derived microglia as compared to saline-encapsulating NPs (Saline-NPs) (Fig. 1D).

#### 3.2. Acute therapeutic effects of MP-NPs on injured spinal cord

MP-NPs locally delivered onto lesioned spinal cord significantly reduced the reactivity of pro-apoptotic proteins (Calpain, iNOS, and Bax), and significantly increased reactivity of anti-apoptotic protein (Bcl-2) at the lesion site when compared to the control treatments. These control treatments included a) Saline-NP, b) locally delivered single dose MP solution (400  $\mu$ g/animal without nanoparticles), Single-MP (see Section 2), and c) systemically delivered high-dose

MP (MP-sys – 30 mg/kg body weight, 7–8 mg MP/animal) (Fig. 2). Expression of early markers of secondary injury was evaluated by semi-quantitative immunofluorescence analysis and Western blot analysis. Using methods published earlier [15], semi-quantitative immunofluorescence analysis was used to determine the spatial distribution and expression level of Calpain, iNOS, Bcl-2 and Bax at and around the lesion site (Fig. 2A and B). Western blot analysis was used to further validate the semi-quantitative immunofluorescence analysis (Fig. 2E). The boundaries of the lesion site were determined by GFAP staining at 24 h and 2 weeks after injury. Two weeks after injury dramatic tissue loss was observed as compared to 24 h after injury, indicating that injury-induced secondary injury followed the initial injury to the spinal cord (Fig. 2C and D).

A semi-quantitative immunofluorescence comparison of Calpain (ubiquitous Ca<sup>2+</sup>-dependent cysteine proteases that cleave cytoskeletal and myelin proteins) expression between experimental groups at 24 h shows that 1) the injury increased Calpain expression in all experimental groups (compared with Calpain expression in uninjured control animals) and 2) MP-NP local delivery significantly reduced the Calpain expression at the lesion site as compared to other experimental groups 24 h after injury (Fig. 2F–J). Besides Calpain, MP-NP treatment also significantly reduced iNOS (a key mediator of inflammation and neurotoxic effects [18]) expression 24 h after injury compared with other groups (Fig. 2K–O).

A comparison of Bcl-2 (an anti-apoptotic protein) and Bax (a pro-apoptotic protein) expression at 24 h demonstrated that MP treatment either by MP-NP or MP-sys, but not by Single-MP

injection, significantly increased Bcl-2 expression, and reduced Bax expression as compared to Saline-NP-treated animals (Fig. 2P–Y). Significantly, MP-NP local treatment was more effective than MP-sys. The ratio of Bcl-2 to Bax, determined by semi-quantitative immunofluorescence comparison (Fig. 2T and Y), is known as a key determinant of neuronal commitment to apoptosis [19]. Bcl-2/Bax was increased in both MP-NP and MP-sys compared with Single-MP and Saline-NP (Fig. 2T and Y), indicating that MP treatment reduced the mitochondria-mediated cell death pathway. At 24 h post-injury, MP-NP local treatment resulted in a higher Bcl-2/Bax ratio than did MP-sys, while there was no significant difference between Single-MP and Saline-NP. These results suggest that sustained MP delivery (accomplished by slow release MP-NP) is required to reduce the reactivity of the injury-related proteins. In addition, Bcl-2<sup>+</sup> neurons were observed at the lesion site in MP-NP-treated animals (Fig. 2P inset).

### 3.3. MP-NP-mediated reduction in lesion volume

MP-NPs delivered locally at the site of spinal cord injury significantly reduced the lesion volume (or spared tissue) compared to the delivery of Saline-NP, Single-MP, or MP-sys at both 2 weeks and 4 weeks after injury. A comparison of GFAP and NF160 double immunostained spinal cord tissue at both 2 and 4 weeks after injury shows that 1) the lesion boundary (i.e., GFAP<sup>+</sup>

astroglial scar delineating lesion) at the 2 weeks' time point was extended beyond the original lesion boundary at 24 h in all experimental groups (Figs. 2 and 3) and 2) the lesion volume was significantly reduced in MP-NP-treated animals as compared to other treatment groups (Fig. 3H). In MP-NP-treated groups, the lesion volume was approximately 50% smaller at both 2 and 4 weeks after injury ( $0.52 \pm 0.1 \text{ mm}^3$  and  $0.61 \pm 0.06 \text{ mm}^3$ , respectively) as compared to groups treated with Saline-NP ( $1.3 \pm 0.1 \text{ mm}^3$  and  $1.2 \pm 0.2 \text{ mm}^3$ ), Single-MP ( $1.3 \pm 0.1 \text{ mm}^3$  at 2 weeks), and MP-sys ( $1.0 \pm 0.11 \text{ mm}^3$  and  $1.2 \pm 0.08 \text{ mm}^3$ ) (Fig. 3H). Interestingly, some NF160<sup>+</sup> axons at 4 weeks in MP-NP-treated groups were observed at the dorsal caudal side, adjacent to the lesion site, and the dorsal rostral side (Fig. 3E and 3<sub>1</sub> and 3<sub>2</sub>). These NF160<sup>+</sup> axons were not observed in Saline-NP and MP-sys-treated groups (Fig. 3F, G, and 3<sub>3–5</sub>). In Saline-NP, Single-MP, and MP-sys-treated animals, many fragmented NF160<sup>+</sup> axons were observed in the lesion core.

### 3.4. MP-NP-mediated reduction in injury-related cellular markers

Local MP-NP treatment significantly reduced the reactivity of GFAP<sup>+</sup> astrocytes, CSPG deposition, and ED-1<sup>+</sup> macrophages/reactive microglia at the lesion site both 2 weeks and 4 weeks after injury (Figs. 4 and 5). A comparison of GFAP and CSPG reactivity between experimental groups demonstrated that the highest

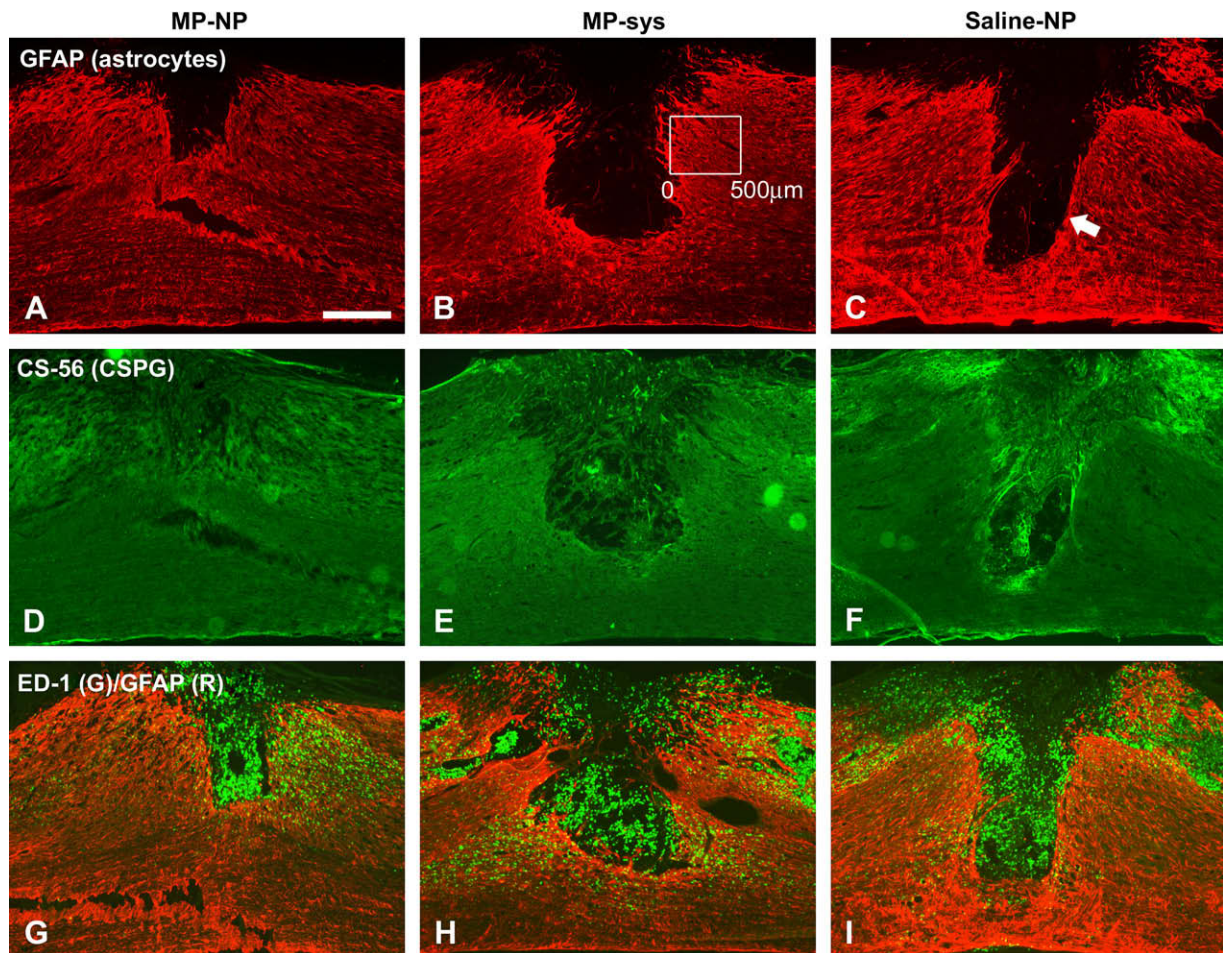


**Fig. 4.** Local MP-NP treatment significantly reduces injury-related cellular markers. A–C) Representative GFAP immunostained (longitudinally sectioned) spinal cord tissue: (A) MP-NP, (B) MP-sys, and (C) Saline-NP-treated animals. Scale bar = 500 µm. D–F) Representative CSPG immunostained spinal cord tissue: (D) MP-NP, (E) MP-sys, and (F) Saline-NP-treated animals. G–I) Representative ED-1 (a marker for macrophages/reactive microglia, green) and GFAP (red) double immunostained spinal cord tissue: (G) MP-NP, (H) MP-sys, and (I) Saline-NP-treated animals.

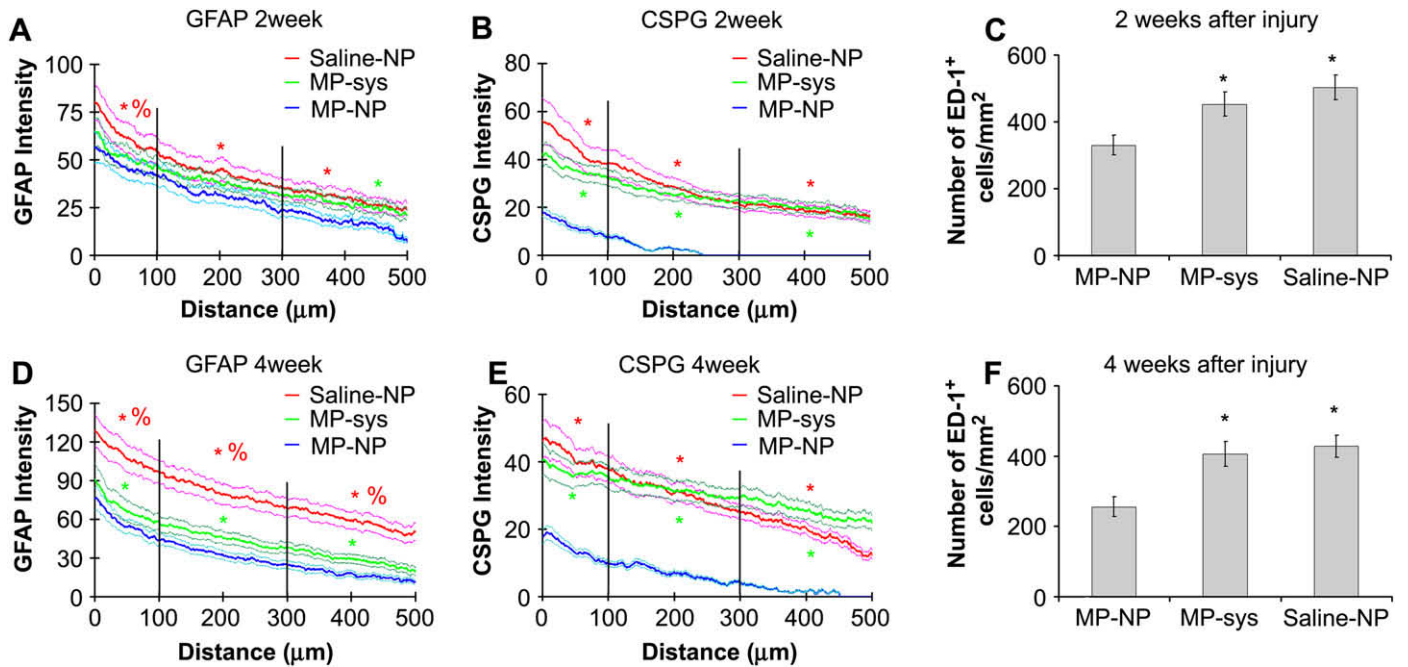


**Fig. 5.** Semi-quantification of injury-related cellular markers. A and D) A quantitative comparison of the averaged intensity of GFAP immunoreactivity between experimental groups shown as the average intensity (thick line) ± s.e.m. (thin line) at 2 weeks (A) and 4 weeks (D) after injury. The Y-axis represents relative GFAP intensity and the X-axis represents a distance from interface between GFAP<sup>+</sup> astroglial scar and lesion core (indicated by the white box in Fig. 4B and the arrow in Fig. 4C). Background subtraction using intact GFAP immunoreactivity was performed. The statistical average intensity difference (summation of the area under the curve) was determined for three different distances: 0–100 μm, 100–300 μm, and 300–500 μm. B and E) A quantitative comparison of the averaged intensity of CSPG immunoreactivity between experimental groups at 2 weeks (B) and 4 weeks (E) after injury. Background subtraction using secondary antibody controls was performed. C and F) A quantitative comparison of the averaged ED-1<sup>+</sup> cells/mm<sup>2</sup> between experimental groups at 2 weeks (C) and 4 weeks after injury (F). \**P* < 0.05 between MP-NP and others. %*P* < 0.05 between MP-sys and Saline-NP.

intensity of GFAP and CSPG reactivity was observed at the interface between lesion core, consisting of infiltrated Vimentin<sup>+</sup> cells (Supplementary data) and ED-1<sup>+</sup> cells, and reactive (hypertrophic with thick processes) astrocytes, forming a dense glial scar. Immunofluorescence intensity gradually decreased with distance from the lesion in all experimental groups (Fig. 5A, B, D, and E).

The lesion core was filled with ED-1<sup>+</sup> macrophages/reactive microglia and Vimentin<sup>+</sup> cells (e.g., fibroblasts) in all experimental groups (Supplementary data and Fig. 4G–I). This histological observation suggests that MP treatment either by local MP-NP or by MP-sys does not abolish the lesion core formation. However, MP-NP treatment dramatically reduced the number of ED-1<sup>+</sup> macrophages/reactive microglia (Fig. 5C and F), suggesting that locally delivered MP might diminish the pro-inflammatory response. The lesion core of all experimental groups was surrounded by GFAP<sup>+</sup> and Vimentin<sup>+</sup> astrocytes (presumably reactive astrocytes, indicated by yellow,

Supplementary data), followed by GFAP<sup>+</sup> but Vimentin<sup>-</sup> astrocytes (indicated by red). The reactive astrocytes close to the lesion core appeared hypertrophic and elongated with thick processes, whereas astrocytes presented further away were typically stellate shaped with thin processes. In Saline-NP-treated animals, more intense and extensive GFAP<sup>+</sup> and Vimentin<sup>+</sup> reactive astrocytes were observed at the lesion site as compared to MP-NP and MP-sys-treated animals (Supplementary data). These results suggest that MP treatment either by MP-NP or by MP-sys reduced the number of GFAP<sup>+</sup> and Vimentin<sup>+</sup> reactive astrocytes at the lesion site.

3.5. MP-NP treatment mediated functional improvement

Fig. 6A and B demonstrates the results of grid and beam walking tests at three different time points: 1, 2, and 4 weeks after injury. In the grid walking test, MP-sys-treated animal groups performed

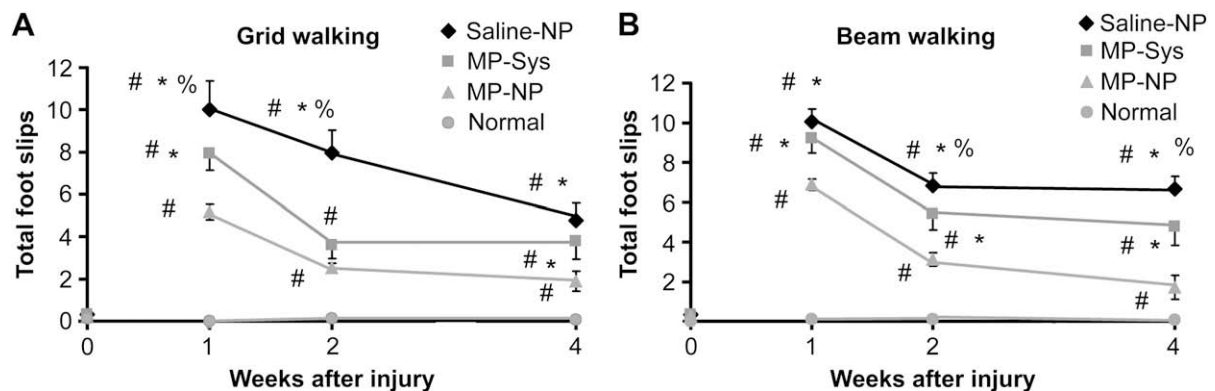


**Fig. 6.** Behavioral assessment. A and B) A quantitative comparison of two different behavioral assessments between treatment groups at three different time points: 1, 2, and 4 weeks after injury: Grid walking (A) and Beam walking (B). Error bars represent s.e.m. #*P* < 0.05 between normal and others. \**P* < 0.05 between MP-NP and others. %*P* < 0.05 between MP-sys and Saline-NP.

significantly better than the Saline-NP-treated animals at 1 and 2 weeks, but not at 4 weeks. MP-NP treatment produced significantly improved functional outcomes as early as 1 week after injury. In the beam walking test, MP-NP-treated groups performed significantly better than both the other two groups at all time points.

#### 4. Discussion

In both human and animal studies, high-dose MP systemic delivery (30 mg/kg bolus injection followed by a 5.4 mg/kg/h infusion over 23 h) has been shown to improve outcomes after spinal cord injury [5,20]. Many studies have demonstrated the effects of systemic MP delivery in the injured spinal cord, including 1) the scavenging of free radicals, which inhibits lipid peroxidation of cell membranes [21], 2) attenuation of apoptotic cell death [22], 3) the decrease in expression of cytokines such as tumor necrosis factor alpha (TNF- $\alpha$ ) and iNOS [23], 4) the inhibition of pro-inflammatory transcription factors, such as NF- $\kappa$ B and AP-1 [24], 5) reduction in the number of ED-1<sup>+</sup> macrophages/microglia at the lesion site [20], and 6) suppression of intracellular Ca<sup>2+</sup>-dependent, Calpain-mediated degradation of neurofilaments and myelin proteins [25]. However, the use of high-dose MP through intravenous administration in acute SCI has become controversial due to the risk of serious side effects. It is reasonable to speculate that most of the side effects of high-dose MP therapy pertain to the high systemic dosage and associated toxicity and that the modest neurological gains are a reflection of inefficient dosing to the injury site. Additionally, a continuous infusion system can introduce the possibility of infections and injuries to the cord associated with the presence of an indwelling catheter.

We have developed and introduced a novel approach for local and sustained MP delivery onto the injured spinal cord tissue through the use of biodegradable polymer-based nanoparticles. MP diffusion in the spinal cord has recently been characterized [28]. Potential advantages of MP-NP local delivery over conventional systemic delivery are as follows: 1) Better therapeutic effect: The sustained and local delivery of MP demonstrates significantly improved therapeutic effects on the injured spinal cord as compared to systemic MP delivery. 2) More efficient, targeted delivery to the injury site: The MP delivery via systemic administration is influenced by the short pharmacokinetic half-life of intravenous MP (2.5–3 h) [26] and P-glycoprotein-mediated exclusion of MP from the spinal cord [27]. Thus, systemic delivery necessitates a high-dose MP regimen, which results in adverse high-dose-associated side effects. We used a significantly lower dose of nanoparticle-encapsulated MP (approximately 400  $\mu$ g/animal) and delivered this dose locally onto the target tissue. This local delivery method significantly enhanced the therapeutic effectiveness of MP by increasing the local dose levels at the target site. 3) Potential to adjust delivery rate or duration: since the MP release profile from nanoparticles can be controlled through the composition of the biodegradable polymer, the rate, amount, or duration of delivery can be adjusted. We expect that this level of control will allow us to further optimize the MP delivery onto lesion site. 4) Injectable and lyophilized fine (submicron) powder formulation: unlike cell-based therapies, MP-NPs can be stored as a lyophilized fine powder. This powder was stored at  $-20^{\circ}\text{C}$  until use, then easily suspended in saline or embedded in hydrogel and locally delivered onto the lesion site.

Our data clearly demonstrate that sustained local delivery of MP-NPs soon after spinal cord injury significantly decreased the reactivity of the early markers of injury/secondary injury, reduced lesion volume, and improved functional outcomes after spinal cord injury. These results were obtained using a remarkably low dose of MP (400  $\mu$ g/animal). The dosage used was approximately 1/20th of

the systemically administered dose (7–8 mg/animal). The sustained and local delivery of MP onto the lesion site enabled by MP-NP treatment generated benefits apparent within the first 24 h after injury (i.e., significantly increased expression of anti-apoptotic protein along with decreased expression of pro-apoptotic related proteins). By comparing the MP-NP group to the Single-MP and Saline-NP groups, it is clear that sustained release of MP was important and that the polymeric particles themselves had no effect. In the long term, MP-NP treatment significantly reduced lesion volumes and this effect was accompanied by significant reductions of injury-related cellular (i.e., astrocytes and macrophages/reactive microglia) reactivity.

#### 5. Conclusion

MP-NP enabled localized and sustained release of MP to the injured spinal cord decreased lesion volume and improved behavioral recovery relative to systemic MP delivery. Based on our results, we suggest that local MP-NP delivery can minimize the side effects associated with high-dose MP systemic dosage, while maximizing the therapeutic effectiveness of MP for treating a spinal cord injury.

#### Acknowledgements

Funding for this research project was provided by GTEC, an NSF funded Engineering Research Center at Georgia Institute of Technology and Emory University, and NIH (R01 NS43486 to RVB). The authors thank Prof. Robert H. Lee, Douglas E. Swehla, Isaac Clements, Efsthios Karathanasis, Anjana Jain, Michael Tanenbaum, and Hyun-Jung Lee for technical discussions and other assistance. The authors also thank Prof. Robert McKeon, Emory University, for useful discussions and assistance in the development of the dorsal over-hemisection animal model of SCI.

#### Appendix

Figures with essential colour discrimination. The majority of the figures in this article may be difficult to interpret in black and white. The full colour images can be found in the online version, at doi:10.1016/j.biomaterials.2008.12.077.

#### Appendix. Supplementary data

(A–C) Representative GFAP (red) and Vimentin (green) double immunostained spinal cord tissue at the lesion site: (A) MP-NP, (B) MP-sys, and (C) Saline-NP-treated animals. Yellow represents a positive signal for both Vimentin and GFAP. Supplementary data associated with this article can be found in the online version at doi:10.1016/j.biomaterials.2008.12.077.

#### References

- [1] Baptiste DC, Fehlings MG. Pharmacological approaches to repair the injured spinal cord. *J Neurotrauma* 2006;23:318–34.
- [2] Becker D, Sadowsky CL, McDonald JW. Restoring function after spinal cord injury. *Neurologist* 2003;9:1–15.
- [3] Sekhon LH, Fehlings MG. Epidemiology, demographics, and pathophysiology of acute spinal cord injury. *Spine* 2001;26:S2–12.
- [4] Bracken MB, Shepard MJ, Holford TR, Leo-Summers L, Aldrich EF, Fazl M, et al. Methylprednisolone or tirilazad mesylate administration after acute spinal cord injury: 1-year follow up. Results of the third national acute spinal cord injury randomized controlled trial. *J Neurosurg* 1998;89:699–706.
- [5] Bracken MB, Shepard MJ, Collins WF, Holford TR, Young W, Baskin DS, et al. A randomized, controlled trial of methylprednisolone or naloxone in the treatment of acute spinal-cord injury. Results of the second national acute spinal cord injury study. *N Engl J Med* 1990;322:1405–11.

- [6] Hall ED. The neuroprotective pharmacology of methylprednisolone. *J Neurosurg* 1992;76:13–22.
- [7] Hall ED. Neuroprotective actions of glucocorticoid and nonglucocorticoid steroids in acute neuronal injury. *Cell Mol Neurobiol* 1993;13:415–32.
- [8] Gerndt SJ, Rodriguez JL, Pawlik JW, Taheri PA, Wahl WL, Micheals AJ, et al. Consequences of high-dose steroid therapy for acute spinal cord injury. *J Trauma* 1997;42:279–84.
- [9] Legos JJ, Gritman KR, Tuma RF, Young WF. Coadministration of methylprednisolone with hypertonic saline solution improves overall neurological function and survival rates in a chronic model of spinal cord injury. *Neurosurgery* 2001;49:1427–33.
- [10] Qian T, Guo X, Levi AD, Vanni S, Shebert RT, Sipski ML. High-dose methylprednisolone may cause myopathy in acute spinal cord injury patients. *Spinal Cord* 2005;43:199–203.
- [11] Li Y, Pei Y, Zhang X, Gu Z, Zhou Z, Yuan W, et al. PEGylated PLGA nanoparticles as protein carriers: synthesis, preparation and biodistribution in rats. *J Control Release* 2001;71:203–11.
- [12] Chen ZJ, Gillies GT, Broadus WC, Prabhu SS, Fillmore H, Mitchell RM, et al. A realistic brain tissue phantom for intraparenchymal infusion studies. *J Neurosurg* 2004;101:314–22.
- [13] Motoyoshi A, Nakajima H, Takano K, Moriyama M, Kannan Y, Nakamura Y. Effects of Amphotericin B on the expression of neurotoxic and neurotrophic factors in cultured microglia. *Neurochem Int* 2008;52:1290–6.
- [14] Giuliani D, Baker TJ. Characterization of amoeboid microglia isolated from developing mammalian brain. *J Neurosci* 1986;6:2163–78.
- [15] Jain A, Kim YT, McKeon RJ, Bellamkonda RV. In situ gelling hydrogels for conformal repair of spinal cord defects, and local delivery of BDNF after spinal cord injury. *Biomaterials* 2006;27:497–504.
- [16] Kunkel-Bagden E, Dai HN, Bregman BS. Methods to assess the development and recovery of locomotor function after spinal cord injury in rats. *Exp Neurol* 1993;119:153–64.
- [17] Basu S, Wang X, Gladwin MT, Kim-Shapiro DB. Chemiluminescent detection of S-nitrosated proteins: comparison of tri-iodide, copper/CO/cysteine, and modified copper/cysteine methods. *Methods Enzymol* 2008;440:137–56.
- [18] Hamada Y, Ikata T, Katoh S, Tsuchiya K, Niwa M, Tsutsumishita Y, et al. Roles of nitric oxide in compression injury of rat spinal cord. *Free Radic Biol Med* 1996;20:1–9.
- [19] Qiu J, Nestic O, Ye Z, Rea H, Westlund KN, Xu GY, et al. Bcl-xL expression after contusion to the rat spinal cord. *J Neurotrauma* 2001;18:1267–78.
- [20] Oudega M, Vargas CG, Weber AB, Kleitman N, Bunge MB. Long-term effects of methylprednisolone following transection of adult rat spinal cord. *Eur J Neurosci* 1999;11:2453–64.
- [21] Topsakal C, Erol FS, Ozveren MF, Yilmaz N, Ilhan N. Effects of methylprednisolone and dexamethorphan on lipid peroxidation in an experimental model of spinal cord injury. *Neurosurg Rev* 2002;25:258–66.
- [22] Vaquero J, Zurita M, Oya S, Aguayo C, Bonilla C. Early administration of methylprednisolone decreases apoptotic cell death after spinal cord injury. *Histol Histopathol* 2006;21:1091–102.
- [23] Xu J, Fan G, Chen S, Wu Y, Xu XM, Hsu CY. Methylprednisolone inhibition of TNF-alpha expression and NF-kB activation after spinal cord injury in rats. *Brain Res Mol Brain Res* 1998;59:135–42.
- [24] Xu J, Kim GM, Ahmed SH, Xu J, Yan P, Xu XM, et al. Glucocorticoid receptor-mediated suppression of activator protein-1 activation and matrix metalloproteinase expression after spinal cord injury. *J Neurosci* 2001;21:92–7.
- [25] Banik NL, Matzelle D, Terry E, Hogan EL. A new mechanism of methylprednisolone and other corticosteroids action demonstrated in vitro: inhibition of a proteinase (calpain) prevents myelin and cytoskeletal protein degradation. *Brain Res* 1997;748:205–10.
- [26] Antal EJ, Wright 3rd CE, Gillespie WR, Albert KS. Influence of route of administration on the pharmacokinetics of methylprednisolone. *J Pharmacokinetic Biopharm* 1983;11:561–76.
- [27] Koszdin KL, Shen DD, Bernards CM. Spinal cord bioavailability of methylprednisolone after intravenous and intrathecal administration: the role of P-glycoprotein. *Anesthesiology* 2000;92:156–63.
- [28] Chvatal SA, Kim Y-t, Bratt Leal AM, Lee H, Bellamkonda RV. Spatial distribution and acute anti-inflammatory effects of methylprednisolone after sustained local delivery to the contused spinal cord. *Biomaterials* 2008;29:1967–75.